Article:
Lin, Z., Wang, Y., Wang, Y.-R. et al. (2024) Photonic crystal enhanced light emitting diodes fabricated by single pulse laser interference lithography. Journal of Applied Physics, 136. 123104. ISSN: 0021-8979

https://doi.org/10.1063/5.0215529

Journal of Applied Physics

RESEARCH ARTICLE | SEPTEMBER 23 2024

Photonic crystal enhanced light emitting diodes fabricated by single pulse laser interference lithography

Zhiheng Lin ; Yaoxun Wang ; Yun-Ran Wang ; Im Sik Han ; Mark Hopkinson

J. Appl. Phys. 136, 123104 (2024)
https://doi.org/10.1063/5.0215529

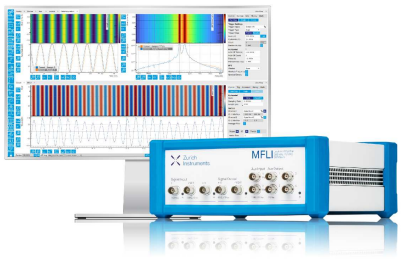

AIP Publishing

Journal of Applied Physics ARTICLE pubs.aip.org/aip/jap

Photonic crystal enhanced light emitting diodes fabricated by single pulse laser interference lithography

Cite as: J. Appl. Phys. **136**, 123104 (2024); doi: 10.1063/5.0215529
Submitted: 31 May 2024 · Accepted: 7 September 2024 ·
Published Online: 23 September 2024

Zhiheng Lin,[a] Yaoxun Wang, Yun-Ran Wang, Im Sik Han, and Mark Hopkinson[b]

AFFILIATIONS

Department of Electronic and Electrical Engineering, The University of Sheffield, Sir Frederick Mappin Building, Sheffield S1 3JD, United Kingdom

[a]**Electronic mail:** ZLIN20@sheffield.ac.uk
[b]**Author to whom correspondence should be addressed:** m.hopkinson@sheffield.ac.uk

ABSTRACT

Integration of photonic crystal (PhC) configurations onto the surfaces of light-emitting diodes (LEDs) can play an important role in enhancing light extraction efficiency. While the literature is rich with various PhC fabrication approaches, there is a need for high throughput methods that are appropriate for low-cost devices. In this paper, we report the use of single pulse laser interference lithography (LIL) for the fabrication of photonic crystal structures on LEDs. The use of brief nanosecond pulse exposures offers significant benefits for high-throughput production. In our study, we have applied single pulse LIL on GaAs/AlGaAs LED structures to achieve high-quality photoresist arrays and then have used inductively coupled plasma etching to create nanoholes into the epitaxial structure. The resulting array forms an effective PhC, controlling surface transmission. Electroluminescence (EL) analyses confirm that these structures enhance the average EL intensity of the LED by up to 3.5 times at room temperature. This empirical evidence underscores the efficacy and potential of this fabrication approach in advancing the functional capabilities of semiconductor-based light-emitting devices.

I. INTRODUCTION

Photonic crystal (PhC) structures are increasingly recognized for their potential to enhance the light performance of light-emitting devices, such as light-emitting diodes (LEDs),[1,2] organic light-emitting diodes (OLEDs),[3] and laser diodes (LDs).[4,5] Within the expansive realm of light-emitting devices, the basic LED as a ubiquitously utilized technology has garnered considerable interest from the research community. This attention is attributed to a multitude of advantages associated with LEDs, including their energy efficiency, and extended operational lifespan. In addition, LEDs are employed in a diverse array of applications such as lighting,[6,7] infrared illumination,[8–10] display technology,[11–13] quantum computation,[14,15] and telecommunications.[16–18] However, despite high internal quantum efficiency, the external radiation efficiency of conventional LEDs is characteristically limited to just a few percent.[19] A significant factor in this is light trapping due to the high refractive index of the semiconductor material. This accentuates the imperative need for advancements in the light extraction efficiency (LEE) of LEDs.[20] This inefficacy in energy utilization represents a substantial wastage, underscoring the urgency for innovation in this domain.

In the pursuit of increasing the light output efficiency of LEDs, the scientific community has embarked on diverse research including meta-surfaces,[21,22] patterned electrodes,[23,24] and various epitaxial growth modifications.[25,26] Each of these technologies possesses the capability to enhance the light-emitting properties of LEDs to varying levels. However, the costs involved resulting from intricate procedural requirements are generally not appropriate for such low-cost devices. PhC structures have emerged as a beneficial alternative to other enhancement methods for increasing the luminous efficacy of LEDs, primarily through the manipulation of light propagation via periodic nanostructuring. This method offers control over the extraction efficiency, spectral purity, and the

direction of light, while requiring no special underlying device scheme.[27,28]

A critical aspect of PhCs is the potential presence of a photonic bandgap (PBG), which delineates a specific range of wavelengths that are prohibited from propagating through the crystal. This results in selective wavelength blocking or transmission control, which also enables the filtration of undesirable spectral components.[19]

Several techniques have been applied for the fabrication of PhC structures on LEDs including conventional UV lithography,[29] electron beam lithography (EBL),[30,31] and nanoimprint lithography (NIL).[32,33] While these methodologies are capable of fabricating nanopatterns with heightened precision, they are associated with considerable financial expenditure and low throughput. In contrast, laser interference lithography (LIL) sets itself apart in nanofabrication with its unique maskless and wide area patterning, presenting a cost-effective alternative compared to traditional methods. Additionally, LIL is distinguished by its capacity for rapid fabrication, a crucial attribute in accelerating the production cycle. The technique is relatively easy to scale by beam expansion and is compatible with step and repeat patterning, which further bolsters its suitability for large-scale industrial manufacturing. Some research studies have explored the use of CW or multi-pulse LIL to integrate PhC structures onto LEDs, resulting in a significant enhancement of their luminous efficiency.[34–36] However, it is noteworthy that these results do not use single-pulse LIL and generally produce structures of micrometer or sub-micrometer pitch, which then operate on higher order reflections.

Our approach is focused on the application of single-pulse LIL to produce structures with sub-500 nm pitch and features (e.g., walls between holes) with sub-100 nm sizes. Using a single nanosecond pulse exposure there is the potential to develop a cost-effective, high-throughput manufacturing technique. Coupled with a fast step and repeat stage, there would be the possibility to rapidly pattern whole LED wafers in a fast timescale and without the requirements of very high vibrational stability.

In this research, we employ a three-beam single pulse LIL arrangement to construct PhC structures of varying depths on GaAs/AlGaAs multiple-quantum-well (MQW) LED samples. Three-beam LIL is used here to avoid the issue of moiré patterns that often emerge from symmetric arrangements such as four beam. Moiré manifests itself in a long-range variation of contrast, which is problematic for uniform resist exposure.[37] Following photoresist exposure and development, we utilize inductively coupled plasma (ICP) etching to create deep nanohole arrays. To aid the analysis, finite-difference-time-domain (FDTD) simulations using Lumerical software have been conducted to calculate the PBG properties and to ascertain the impact of various PhC depths on LEE enhancement.

II. DESIGN OF PHC STRUCTURE

The LED samples in this study were fabricated using molecular beam epitaxy (MBE) on n-type GaAs substrates. The structure of the LED comprises a sequential layering, starting with a 400 nm n-doped GaAs buffer layer and followed by a 1300 nm n-doped Al0.3Ga0.7As confinement layer. The active region features three 9 nm thick GaAs Quantum Wells (QWs), each separated by 24 nm thick Al0.3Ga0.7As barriers. Above this, an 800 nm p-doped Al0.3Ga0.7As upper confinement layer is placed, and the structure is capped with a 20 nm p-doped GaAs layer, forming the device's topmost section.

This study focuses on GaAs-based LEDs emitting around 850 nm at room temperature, necessitating PhC structures that enhance gain within this wavelength range. The simulation by FDTD can help us to find the suitable pitch size for the PhC structures.

Figure 1 illustrates the outcomes of a PBG simulation using the FDTD method (Ansys Lumerical). The dispersion diagram demonstrates the formation of a PBG in two spectral regions, specifically from normalized frequencies of 0.28–0.31 and 0.38–0.44. Using a pitch of 365 nm, this corresponds to PBGs at wavelengths of 830–960 nm and 1177–1303 nm. With these regions, the 2D PhC structure will serve as an efficient out-coupler for transverse electric (TE) guided modes, a crucial aspect for enhancing the performance of our LED samples.

The shape of the fabricated PhC structure is dictated by the interference pattern, as described by Eq. (1). Equation (2) establishes the relationship between the pitch (P) of the interference pattern and the angle of incidence (θ) of the laser beams,

$$I = \left| \sum_{i=1}^{n} A_m \overrightarrow{P_m} \exp\left[i\left(\overrightarrow{k_m} \cdot \vec{r} + \delta_m \right) \right] \right|^2, \tag{1}$$

$$P = \frac{\lambda}{\sqrt{2}\,\sin\,\theta}. \tag{2}$$

The formation of the pattern using a three-beam LIL configuration was simulated using plane wave approximation in MATLAB. This simulation is crucial for the conceptualization and planning of the PhC structure fabrication process. Figure 2 shows a simulation of the laser intensity distribution pattern for the LIL arrangement we have used.

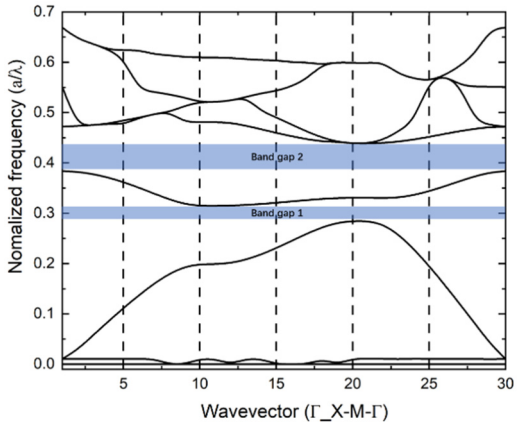

FIG. 1. The PBG for the 2D PhC obtained from FDTD calculations.

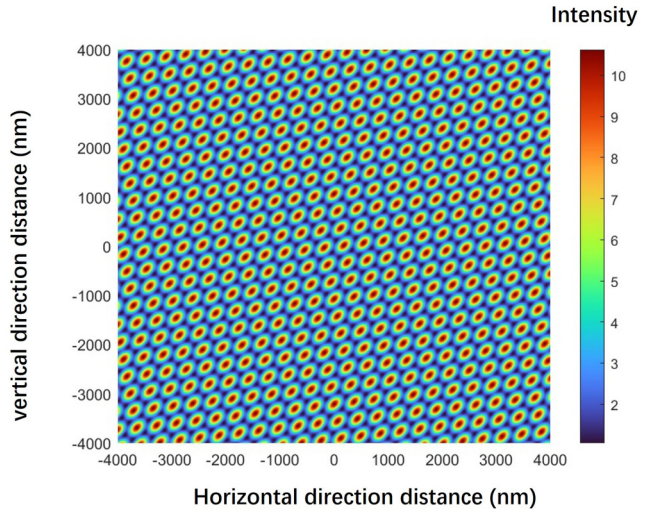

FIG. 2. Laser interference pattern simulation.

III. FABRICATION PROCESS OF THE PHC STRUCTURE

Figure 3 illustrates the process of preparing the LED samples. In this study, the centerpiece of our experimental setup is the LIL system, powered by a flashlamp pumped Nd: YAG laser. This laser is notable for its precise operational characteristics: it emits at a wavelength of 355 nm, with a repetition rate of 5 Hz, a pulse duration of 7 ns, and a beam width of 5 mm. Single pulses are selected using a mechanical shutter. Through the strategic deployment of beam splitters and mirrors, we partition the laser output into four identical beams, with three converging accurately at the same point on the sample. This precise alignment is crucial for the objectives of our study.

The preparation of LED samples commenced with a three-step cleaning protocol. Following a pre-bake step, the substrates were coated with a 180 nm thick layer of mr-P 1200LIL photoresist (Micro resist Technology GmbH). This photoresist is tailored for laser lithography applications, offering high contrast even at reduced film thicknesses, which is essential for precise patterning. It is pertinent to acknowledge that the depth of photoresist exposure can be achieved by varying the laser pulse energy using an attenuator. However, an increase in the laser energy to expose deeper layers of the photoresist brings with it the risk of laser-induced damage (dissociation and delamination). Consequently, the employment of a thin, high-contrast photoresist is strategically advantageous as it enables complete etching with lower-energy single pulses.

After applying the photoresist, the sample underwent single 7 ns exposure of three-beam LIL to create the PhC pattern. The pitch of this pattern is adjustable via the laser beams' angle of incidence. In this setup, the angle of incidence of three beams is set to be 43°, and the azimuth angles are set at 0°, 90°, and 180°, respectively. Furthermore, to prevent damage to the PhC pattern, a careful balance of laser energy is required, with 9 mJ being the chosen parameter. Following this, the exposed sample is developed in a metal bearing, silicate/phosphate-based developer (ma-D 374/S- Microresist technology GmbH) for a duration of 20–40 s.

Pattern transfer from the photoresist mask was achieved through ICP etching using a Cl/Ar chemistry (Oxford instrument Plasmapro). The etching rate was maintained at 200 nm/min. By adjusting the etching time, PhC structures of various depths were fabricated. These depths all lie within the 800 nm p-type top layer of the epitaxial structure. After solvent removal of the photoresist, we obtain a PhC structure with an elliptical hole shape, as depicted in the Scanning Electron Microscopy (SEM) images in Fig. 4. In these images, the major axis of the ellipse has an approximate diameter of 315 nm and the minor axis is around 305 nm. The pitch size is about 365 nm, which aligns with the theoretical

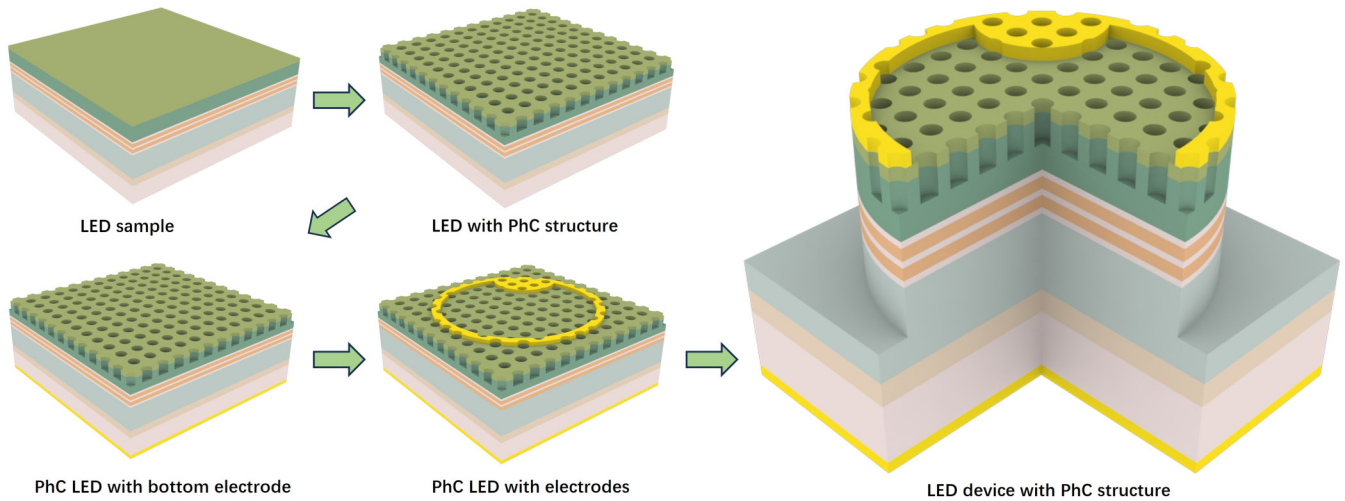

FIG. 3. Fabrication process for the PhC structure on the LED mesa device.

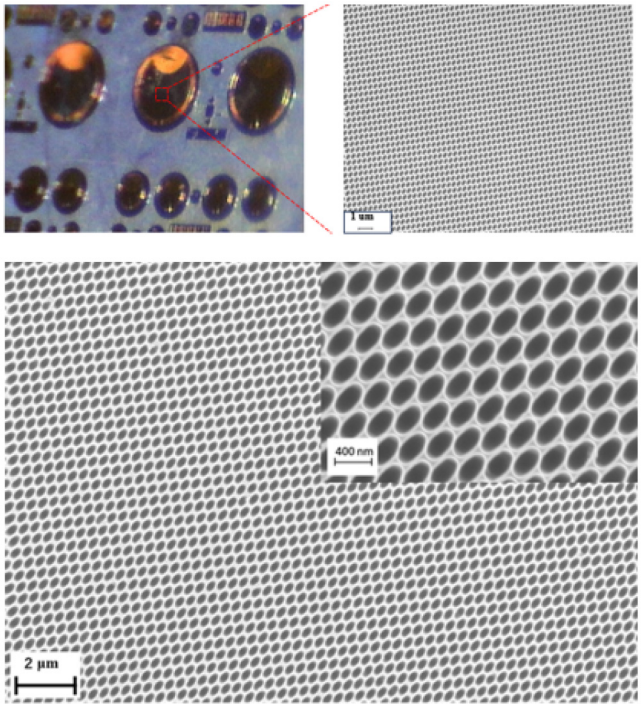

FIG. 4. SEM images of the LED sample with PhC structures.

assessment of PBG required for a device operating wavelength of around 850 nm.

Subsequently, a device metallization process was conducted wherein a 30 nm layer of Ti followed by a 200 nm layer of Au was deposited on both the bottom and top surfaces of the samples. The extraneous metal on the surface was then removed using a lift-off technique, thereby delineating the electrode patterns. The final fabrication stage involved the creation of mesastructures using ICP etching, which resulted in the formation of 400 μm diameter LED devices integrated with PhC structures.

IV. FDTD SIMULATION OF FAR-FIELD ANGULAR DISTRIBUTION PLOTS FOR LEDS

To elucidate the influence of the depth of PhC structures on the LEE gain in LED, a series of FDTD simulations were conducted. These 2D simulations focused on LEDs incorporating PhC structures of varying depths, as visualized in the cross-sectional representations presented in Fig. 5. In our simulation setup, a dipole emitter, serving as a surrogate for the light source, is positioned at the location of the MQW layer. This simulation is to filter out more suitable depth intervals. Since the simulation is only performed over a large range, we will replace the ellipse with a circle with a diameter of 310 nm for the convenience of the experiment.

Figures 6(a)–6(f) present the far-field angular distribution plots for LEDs with varying depths of nanoholes: without a PhC structure (0 nm) and with 100, 200, 300, 400, and 500 nm depths,

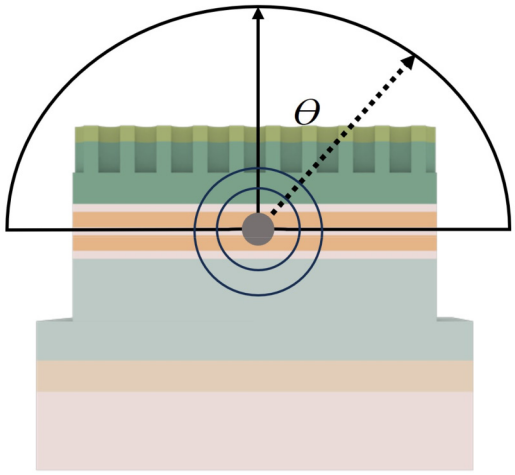

FIG. 5. LED cross-sectional FDTD simulation schematic.

respectively. The color bar symbolizes the intensity of light, the horizontal axis represents the direction of light propagation, and the vertical axis corresponds to the wavelength of the light. It is worth noting that light interacting with the PhC structure exhibits restricted lateral propagation for wavelengths outside the 830 nm to 960 nm range. This phenomenon is more conspicuously delineated in Figs. 6(c)–6(f).

Starting with the unstructured device [Fig. 6(a)], Figs. 6(b) and 6(c) demonstrate that structural depths of 100 and 200 nm fall short of producing an effective photonic bandgap effect and as a result only slight enhancement of the LEE, as illustrated in Fig. 7. Conversely, as illustrated in Fig. 6(d), the optimal depth for PhC structures achieves a balance between effective light manipulation and minimizing losses due to absorption or scattering. This depth effectively utilizes the photonic bandgap effect to enhance the LEE (average 1.3 times), as highlighted in Fig. 7. If we compare this to alternative LEE control methods, such as micropillars, one such study shows a 45% improvement in LEE,[38] indicating that we have a somewhat similar achievement using a simpler fabrication process. However, as Figs. 6(e) and 6(f) indicate, deeper PhC structures, such as those with 400 and 500 nm depths, do not further increase the gain. Instead, they introduce multiple diffraction complexity, leading to destructive interference and the redirection of light at non-optimal angles. These deeper structures create more complex pathways for light, contributing to internal light losses and a reduction in overall light output efficiency. Therefore, while a certain depth is necessary for effective light manipulation, excessively deep PhC structures can be counterproductive, as shown in the limited LEE gain in 400 and 500 nm deep structures in Fig. 6.

V. ELECTROLUMINESCENCE RESULTS

Based on the insights derived from simulation studies, we have concentrated our efforts on depths of around 300 nm for the ICP etched nanoholes. The etching process is executed utilizing a

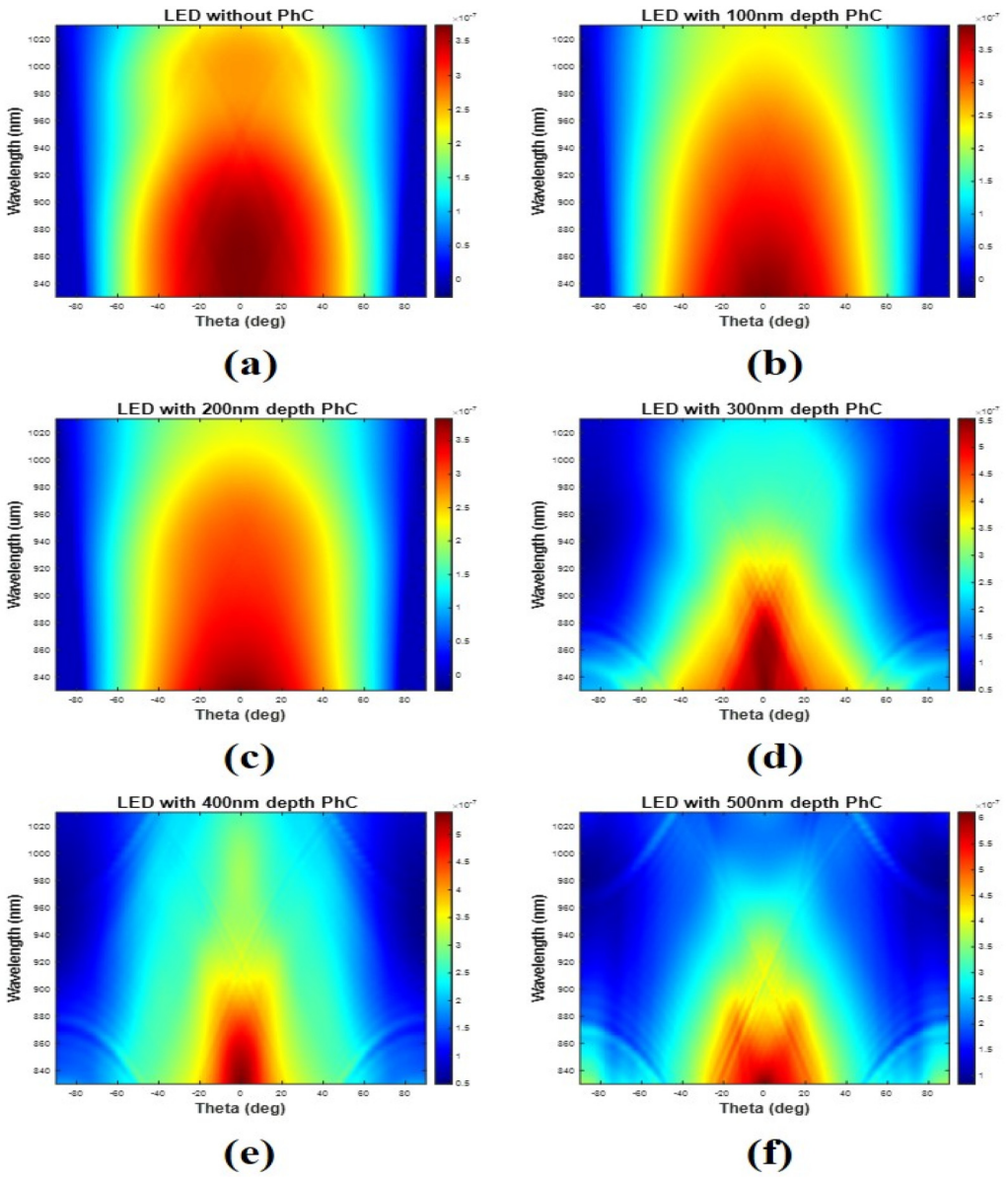

FIG. 6. Far-field angular distribution plots for (a) LED without a PhC structure, (b) 100, (c) 200, (d) 300, (e) 400, and (f) 500 nm depths of PhC structures on LEDs.

gaseous amalgam of SiCl4 and Ar2, achieving a consistent etching rate of 200 nm/min. Given the relatively thin photoresist layer of 180 nm used in our experiment, prolonged etching durations risk compromising the integrity of the PhC structures. Consequently, in this study, the LED samples underwent ICP etching for timed intervals of 60, 70, 80, 90, and 100 s.

To ascertain the impact of varying depths of PhC structures on the LEE of LEDs, EL measurements were conducted. These evaluations encompassed LEDs with PhC structures of differentiated depths as well as control samples devoid of PhC structures. It is crucial to note that the etching depth for the PhC structures was strategically set to be substantially distant from the MQW layer. This distance ensures that the internal quantum efficiency (IQE) of the LEDs is not significantly affected, irrespective of the presence or absence of a PhC structure in the upper capping layer. A comparison of IV curves confirms that the process of integrating PhC structures does not detrimentally impact the diode's electrical performance, as shown in Fig. 8(a).

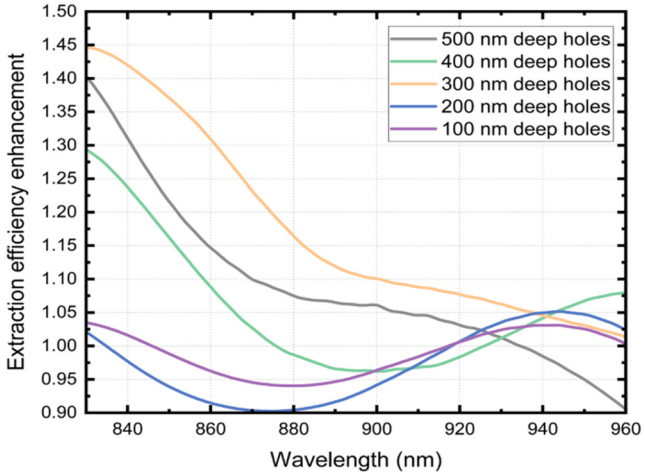

FIG. 7. The relationship between LEE enhancement and wavelength of LEDs with different depth PhC structures.

Figures 8(b)–8(f) present the EL profiles of LEDs featuring PhC structures of varying depths, in comparison with the conventional LED, under distinct injection current conditions (10, 20, 50, 70, 100 mA) at room temperature. EL color fill contour profiles for LEDs incorporating PhC structures with varying depths are provided in the supplementary material. When increasing the injection current into the LED from 10 to 100 mA, a subtle blueshift in the emission wavelength is observed, transitioning from 845 to 850 nm. This phenomenon can predominantly be attributed to the Burstein–Moss shift (BMS).[39]

The enhancements in light intensity observed in the EL measurements are primarily attributed to the improved LEE imparted by the incorporation of the PhC structures. This inference is drawn from the fact that the IQE of the LEDs remains largely invariant, thereby indicating that the augmented EL intensity is a direct consequence of the enhanced light extraction capabilities facilitated by the PhC structures. Figures 8(b)–8(f) corroborate this statement, clearly illustrating a consistent trend where LEDs with PhC structures manifest a higher luminous intensity as compared to their conventional counterparts under equivalent operational conditions. A detailed analysis shown in Fig. 9 reveals that LEDs with a PhC

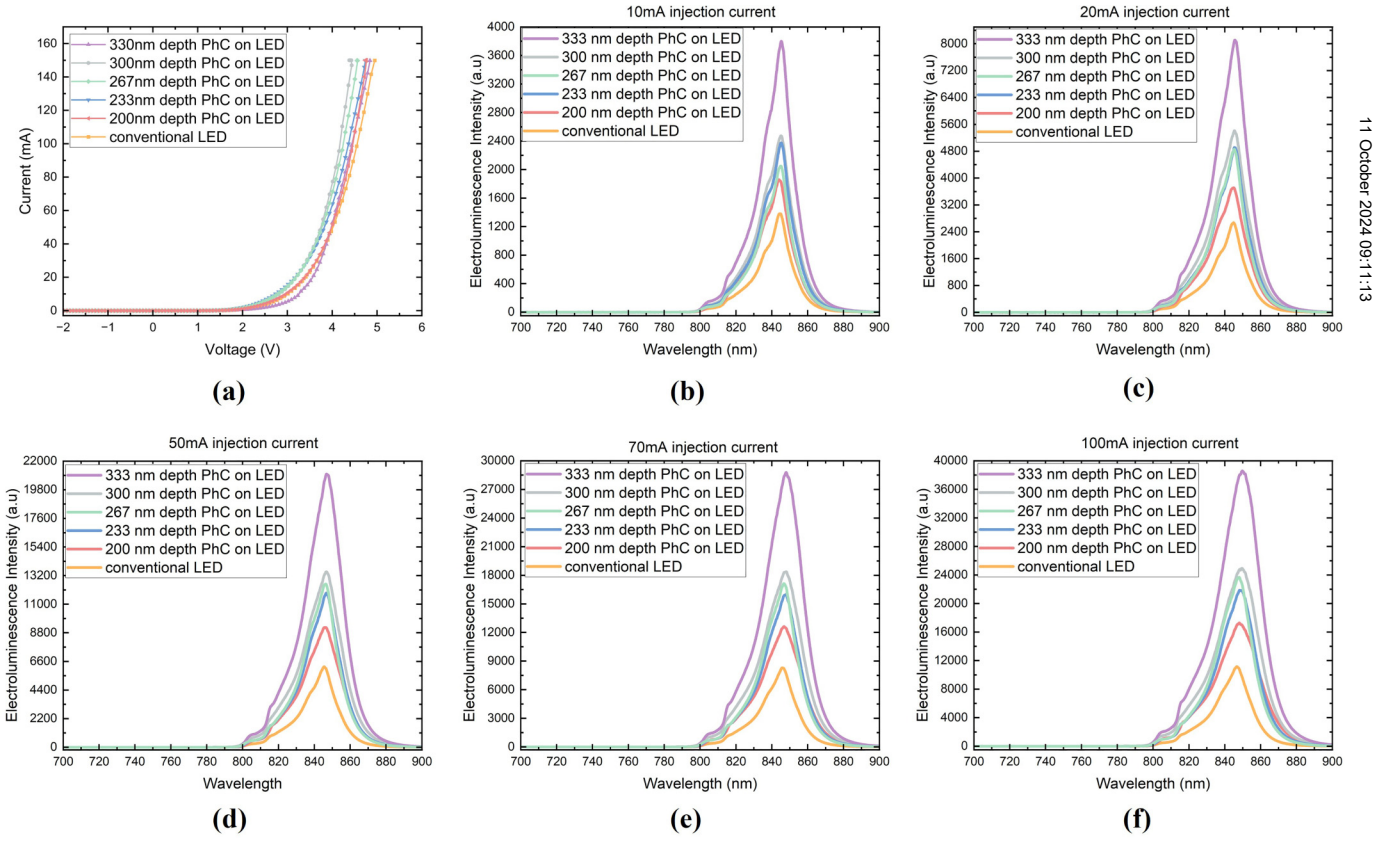

FIG. 8. (a) The IV curves for LEDs with different depth PhC structures, (b) 10, (c) 20, (d) 50, (e) 70, (f) 100 mA injection current EL results for LEDs with different depth PhC structures.

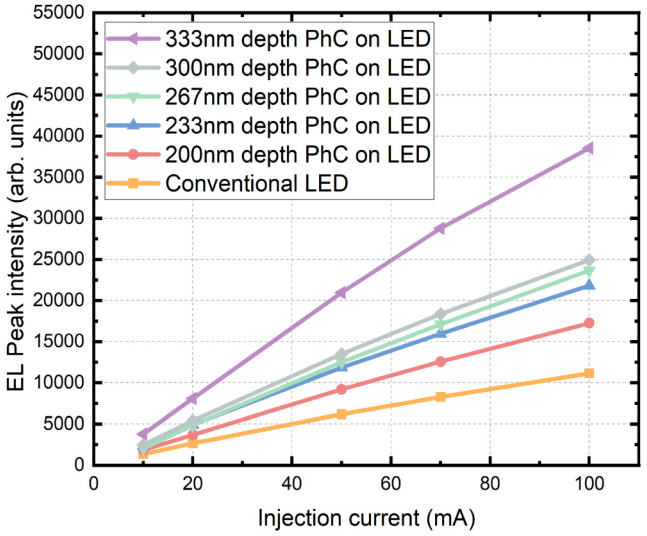

FIG. 9. The relationship between peak position EL intensity and injection current for conventional LED and LEDs with different depth PhC structures.

depth of merely 200 nm display an increase in EL intensity averaging an enhancement of 1.5 times. For PhC structures with depths of 233, 267 , and 300 nm, there is a slow gradual enhancement in the gain of EL intensity, with average increases of 2 times, 2.1 times, and 2.15 times, respectively. Remarkably, at a PhC depth of 333 nm, there is an exponential augmentation in EL intensity, quantified by an average increase factor of 3.5, indicating a substantial impact of PhC depth on the EL efficiency of LEDs.

VI. CONCLUSION

In this work, we have designed and fabricated photonic crystal LED structures using nanosecond pulsed laser interference lithography, coupled with pattern transfer using reactive ion etching. We have investigated the impact of the PhC depth on the LEE of GaAs/AlGaAs MQW LEDs emitting at 850 nm at room temperature. According to the SEM results, high quality PhC structures were successfully crafted on the LED samples using a three-beam single pulse LIL technique and controlled ICP etching to vary the etch depths. FDTD simulations were performed to assess the PBG properties of the PhC structures, verifying their effectiveness in boosting light emission at the desired 850 nm wavelength. Simulations of the LED cross-section structure pinpointed an optimal nanohole depth of around 300 nm for peak LEE gains. This result was validated by EL measurements on LEDs with various PhC depths, with a notable 3.5-fold increase in EL intensity at a 333 nm PhC depth, highlighting a substantial improvement in light emission efficiency.

The study is based on a GaAs-based LED operating at 850 nm as a suitable test bed. Although widely used for infrared illumination, there are of course many other wavelengths and semiconductor materials for which this approach could be applied. The technique is adaptable through re-configuration of the three-beam single-pulse LIL setup and should have a wide capability to enhance the luminous efficacy of LEDs operating at diverse wavelengths. With exposure times in the nanosecond range, it is an inherently high-throughput method to create nanoscale period arrays which if combined with fast step and repeat stages could form a high throughput method for cost-effective fabrication.

SUPPLEMENTARY MATERIAL

See the supplementary material as electroluminescence color fill contour profiles for LEDs incorporating PhC structures with varying depths.

ACKNOWLEDGMENTS

The authors gratefully acknowledge financial support from EPSRC (Grant No. EP/X016838/1) and the Grantham Foundation Opportunities Fund.

AUTHOR DECLARATIONS

Conflict of Interest

The authors have no conflicts to disclose.

Author Contributions

Zhiheng Lin: Formal analysis (lead); Investigation (lead); Methodology (equal); Writing – original draft (lead). **Yaoxun Wang:** Investigation (equal); Methodology (equal). **Yun-Ran Wang:** Conceptualization (equal); Investigation (equal); Supervision (equal); Writing – original draft (equal). **Im Sik Han:** Investigation (equal). **Mark Hopkinson:** Conceptualization (lead); Funding acquisition (equal); Investigation (supporting); Project administration (lead); Supervision (lead); Writing – review & editing (lead).

DATA AVAILABILITY

The data that support the findings of this study are available from the corresponding author upon reasonable request.

REFERENCES

[1]H. Lee, T. Y. Lee, Y. Park, K. S. Cho, Y. G. Rho, H. Choo, and H. Jeon, "Structurally engineered colloidal quantum dot phosphor using TiO_2 photonic crystal backbone," Light Sci. Appl. **11**(1), 318 (2022).
[2]S. M. Ko, J. Hur, C. Lee, Isnaeni, S. H. Gong, M. K. Kim, and Y. H. Cho, "Hexagonal GaN nanorod-based photonic crystal slab as simultaneous yellow broadband reflector and blue emitter for phosphor-conversion white light emitting devices," Sci. Rep. **10**(1), 358 (2020).
[3]D. Allemeier, B. Isenhart, E. Dahal, Y. Tsuda, T. Yoshida, and M. S. White, "Emergence and control of photonic band structure in stacked OLED microcavities," Nat. Commun. **12**(1), 6111 (2021).
[4]K. Emoto, T. Koizumi, M. Hirose, M. Jutori, T. Inoue, K. Ishizaki, M. De Zoysa, H. Togawa, and S. Noda, "Wide-bandgap GaN-based watt-class photonic-crystal lasers," Commun. Mater. **3**(1), 72 (2022).
[5]Y. Yu, W. Xue, E. Semenova, K. Yvind, and J. Mork, "Demonstration of a self-pulsing photonic crystal Fano laser," Nat. Photonics **11**(2), 81–84 (2017).
[6]Y.-K. Wang, F. Jia, X. Li, S. Teale, P. Xia, Y. Liu, P. Tsz-shan Chan, H. Wan, Y. Hassan, M. Imran, H. Chen, L. Grater, L.-D. Sun, G. C. Walker, S. Hoogland,

Z.-H. Lu, C.-H. Yan, L.-S. Liao, and E. H. Sargent, "Self-assembled monolayer-based blue perovskite LEDs," Sci. Adv. **9**(36), eadh2140 (2023).
[7]A. M. Nahavandi, M. Safi, P. Ojaghi, and J. Y. Hardeberg, "LED primary selection algorithms for simulation of CIE standard illuminants," Opt. Express **28**(23), 34390 (2020).
[8]X. Shen, A. Kamath, and P. Guyot-Sionnest, "Mid-infrared cascade intraband electroluminescence with HgSe–CdSe core–shell colloidal quantum dots," Nat. Photonics **17**(12), 1042–1046 (2023).
[9]F. Yuan, G. Folpini, T. Liu, U. Singh, A. Treglia, J. W. M. Lim, J. Klarbring, S. I. Simak, I. A. Abrikosov, T. C. Sum, A. Petrozza, and F. Gao, "Bright and stable near-infrared lead-free perovskite light-emitting diodes," Nat. Photonics **18**(2), 170–176 (2024).
[10]M. Ghali, K. Ohtani, Y. Ohno, and H. Ohno, "Generation and control of polarization-entangled photons from GaAs island quantum dots by an electric field," Nat. Commun. **3**, 661 (2012).
[11]Y. Yao, Y. Chen, K. Wang, N. Turetta, S. Vitale, B. Han, H. Wang, L. Zhang, and P. Samorì, "A robust vertical nanoscaffold for recyclable, paintable, and flexible light-emitting devices," Sci. Adv. **8**(10), eabn2225 (2022).
[12]M. Woo Jeong, J. Hyun Ma, J. Seung Shin, J. Su Kim, G. Ma, T. Uk Nam, X. Gu, S. Jun Kang, and J. Young Oh, "Intrinsically stretchable three primary light-emitting films enabled by elastomer blend for polymer light-emitting diodes," Sci. Adv. **9**(25), eadh1504 (2023).
[13]J. Park, J. H. Choi, K. Kong, J. H. Han, J. H. Park, N. Kim, E. Lee, D. Kim, J. Kim, D. Chung, S. Jun, M. Kim, E. Yoon, J. Shin, and S. Hwang, "Electrically driven mid-submicrometre pixelation of InGaN micro-light-emitting diode displays for augmented-reality glasses," Nat. Photonics **15**(6), 449–455 (2021).
[14]C. Couteau, S. Barz, T. Durt, T. Gerrits, J. Huwer, R. Prevedel, J. Rarity, A. Shields, and G. Weihs, "Applications of single photons to quantum communication and computing," Nat. Rev. Phys. **5**(6), 326–338 (2023).
[15]T. K. Hsiao, A. Rubino, Y. Chung, S. K. Son, H. Hou, J. Pedrós, A. Nasir, G. Éthier-Majcher, M. J. Stanley, R. T. Phillips, T. A. Mitchell, J. P. Griffiths, I. Farrer, D. A. Ritchie, and C. J. B. Ford, "Single-photon emission from single-electron transport in a SAW-driven lateral light-emitting diode," Nat. Commun. **11**(1), 917 (2020).
[16]T. Müller, J. Skiba-Szymanska, A. B. Krysa, J. Huwer, M. Felle, M. Anderson, R. M. Stevenson, J. Heffernan, D. A. Ritchie, and A. J. Shields, "A quantum light-emitting diode for the standard telecom window around 1,550 nm," Nat. Commun. **9**(1), 862 (2018).
[17]Y. Zhou, Z. Wang, A. Rasmita, S. Kim, A. Berhane, Z. Bodrog, G. Adamo, A. Gali, I. Aharonovich, and W.-B. Gao, "Room temperature solid-state quantum emitters in the telecom range," Sci. Adv. **4**(3), eaar3580 (2018).
[18]Y. Yu, S. Liu, C. M. Lee, P. Michler, S. Reitzenstein, K. Srinivasan, E. Waks, and J. Liu, "Telecom-band quantum dot technologies for long-distance quantum networks," Nat. Nanotechnol. **18**(12), 1389–1400 (2023).
[19]K. Wang, X. Dong, Y. Bu, and X. Wang, "Design of photonic crystals for light-emitting diodes," J. Am. Ceram. Soc. **106**(12), 7146–7188 (2023).
[20]H. Hu, B. Tang, H. Wan, H. Sun, S. Zhou, J. Dai, C. Chen, S. Liu, and L. J. Guo, "Boosted ultraviolet electroluminescence of InGaN/AlGaN quantum structures grown on high-index contrast patterned sapphire with silica array," Nano Energy **69**, 104427 (2020).
[21]P. Mao, C. Liu, X. Li, M. Liu, Q. Chen, M. Han, S. A. Maier, E. H. Sargent, and S. Zhang, "Single-step-fabricated disordered metasurfaces for enhanced light extraction from LEDs," Light Sci. Appl. **10**(1), 180 (2021).
[22]E. Khaidarov, Z. Liu, R. Paniagua-Domínguez, S. T. Ha, V. Valuckas, X. Liang, Y. Akimov, P. Bai, C. E. Png, H. V. Demir, and A. I. Kuznetsov, "Control of LED emission with functional dielectric metasurfaces," Laser Photon Rev. **14**(1), 1900235 (2020).
[23]J. Chen, T. Wang, and X. Wang, "Enhancing light extraction efficiency of GaN LED by combining complex-period photonic crystals with doping," J. Am. Ceram. Soc. **106**(8), 4752–4769 (2023).
[24]L. Zhou, H. Y. Xiang, S. Shen, Y. Q. Li, J. De Chen, H. J. Xie, I. A. Goldthorpe, L. Sen Chen, S. T. Lee, and J. X. Tang, "High-performance flexible organic light-emitting diodes using embedded silver network transparent electrodes," ACS Nano **8**(12), 12796–12805 (2014).
[25]S. M. Lee, Y. Cho, D. Y. Kim, J. S. Chae, and K. C. Choi, "Enhanced light extraction from mechanically flexible, nanostructured organic light-emitting diodes with plasmonic nanomesh electrodes," Adv. Opt. Mater. **3**(9), 1240–1247 (2015).
[26]M. L. Lee, Y. H. You, R. M. Lin, C. J. Hsieh, V. C. Su, P. H. Chen, and C. H. Kuan, "Utilizing two-dimensional photonic crystals in different arrangement to investigate the correlation between the air duty cycle and the light extraction enhancement of InGaN-based light-emitting diodes," IEEE Photonics J. **6**(3), 1–8 (2014).
[27]T. Sridarshini and S. Indira Gandhi, "Photonic band structure of 2D photonic crystals—A comparative study," Laser Phys. **30**(2), 026205 (2020).
[28]D. Przybylski and S. Patela, "Modelling of a two-dimensional photonic crystal as an antireflection coating for optoelectronic applications," Opto-Electron. Rev. **27**(1), 79–89 (2019).
[29]X. Tang, L. Han, Z. Ma, Z. Deng, Y. Jiang, W. Wang, H. Chen, C. Du, and H. Jia, "Enhanced light extraction from AlGaInP-based red light-emitting diodes with photonic crystals," Opt. Express **29**(4), 5993 (2021).
[30]L. Shterengas, R. Liu, A. Stein, G. Kipshidze, W. J. Lee, and G. Belenky, "Continuous wave room temperature operation of the 2 μm GaSb-based photonic crystal surface emitting diode lasers," Appl. Phys. Lett. **122**(13), 131102 (2023).
[31]S. Hou, A. Xie, Z. Xie, L. Y. M. Tobing, J. Zhou, L. Tjahjana, J. Yu, C. Hettiarachchi, D. Zhang, C. Dang, E. H. T. Teo, M. D. Birowosuto, and H. Wang, "Concurrent inhibition and redistribution of spontaneous emission from all inorganic perovskite photonic crystals," ACS Photonics **6**(6), 1331–1337 (2019).
[32]C. Wang, Y. Fan, J. Shao, Z. Yang, J. Sun, H. Tian, and X. Li, "Discretely-supported nanoimprint lithography for patterning the high-spatial-frequency stepped surface," Nano Res. **14**(8), 2606–2612 (2021).
[33]M. Modaresialam, Z. Chehadi, T. Bottein, M. Abbarchi, and D. Grosso, "Nanoimprint lithography processing of inorganic-based materials," Chem. Mater. **33**(14), 5464–5482 (2021).
[34]D. Pudis, L. Suslik, J. Skriniarova, J. Kovac, J. Kovec, I. Kubicova, I. Martincek, S. Hascik, and P. Schaaf, "Effect of 2D photonic structure patterned in the LED surface on emission properties," Appl. Surf. Sci. **269**, 161–165 (2013).
[35]X. Tang, L. Wang, M. Zhao, W. Huo, L. Han, Z. Deng, Y. Jiang, W. Wang, H. Chen, C. Du, and H. Jia, "Enhancement of light extraction efficiency of AlGaInP-based light emitting diodes by silicon oxide hemisphere array," Opt. Commun. **481**, 126539 (2021).
[36]P. Zuo, B. Zhao, S. Yan, G. Yue, H. Yang, Y. Li, H. Wu, Y. Jiang, H. Jia, J. Zhou, and H. Chen, "Improved optical and electrical performances of GaN-based light emitting diodes with nano truncated cone SiO_2 passivation layer," Opt. Quantum Electron **48**, 1–7 (2016).
[37]Y. R. Wang, I. S. Han, C. Y. Jin, and M. Hopkinson, "Precise arrays of epitaxial quantum dots nucleated by *in situ* laser interference for quantum information technology applications," ACS Appl. Nano Mater. **3**(5), 4739–4746 (2020).
[38]B. Romeira, J. Borme, H. Fonseca, J. Gaspar, and J. B. Nieder, "Efficient light extraction in subwavelength GaAs/AlGaAs nanopillars for nanoscale light-emitting devices," Opt. Express **28**(22), 32302–32315 (2020).
[39]S. Ni, H. Qin, J. Wen, X. Li, M. Li, T. Tang, and F. Liu, "Burstein-Moss shift of lead halide perovskite quantum dots induced by electron injection from graphene oxide," Appl. Surf. Sci. **545**, 149003 (2021).